

Temperature curve of magnetization and left-handed properties of $\text{La}_{0.775}\text{Sr}_{0.225}\text{MnO}_3$

D. P. Belozorov, T. V. Kalmykova, S. I. Tarapov, A. M. Pogorily, A. I. Tovstolytkin et al.

Citation: *Appl. Phys. Lett.* **100**, 171104 (2012); doi: 10.1063/1.4705729

View online: <http://dx.doi.org/10.1063/1.4705729>

View Table of Contents: <http://apl.aip.org/resource/1/APPLAB/v100/i17>

Published by the [American Institute of Physics](#).

Related Articles

Reducing spin torque switching current density by boron insertion into a CoFeB free layer of a magnetic tunnel junction

Appl. Phys. Lett. **100**, 172407 (2012)

Electromagnetic responses of magnetic conductive hollow fibers

J. Appl. Phys. **111**, 084506 (2012)

Reversible switching of room temperature ferromagnetism in CeO_2 -Co nanoparticles

Appl. Phys. Lett. **100**, 172405 (2012)

Switching through intermediate states seen in a single nickel nanorod by cantilever magnetometry

J. Appl. Phys. **111**, 083911 (2012)

Switchable hyperbolic metamaterials with magnetic control

Appl. Phys. Lett. **100**, 161108 (2012)

Additional information on *Appl. Phys. Lett.*

Journal Homepage: <http://apl.aip.org/>

Journal Information: http://apl.aip.org/about/about_the_journal

Top downloads: http://apl.aip.org/features/most_downloaded

Information for Authors: <http://apl.aip.org/authors>

ADVERTISEMENT

| INSTRUMENTS FOR ADVANCED SCIENCE | | | | |
|--|--|--|---|--|
|  | Gas Analysis dynamic measurement of reaction gas streams catalysis and thermal analysis molecular beam studies dissolved species probes fermentation, environmental and ecological studies | Surface Science UHV TPD SIMS end point detection in ion beam etch elemental imaging - surface mapping | Plasma Diagnostics plasma source characterisation etch and deposition process reaction kinetic studies analysis of neutral and radical species | Vacuum Analysis partial pressure measurement and control of process gases reactive sputter process control vacuum diagnostics vacuum coating process monitoring |
| |  |  |  |  |
| <p>contact Hiden Analytical for further details: info@hiden.co.uk www.HidenAnalytical.com CLICK TO VIEW OUR PRODUCT CATALOGUE</p> | | | | |

Temperature curve of magnetization and left-handed properties of $\text{La}_{0.775}\text{Sr}_{0.225}\text{MnO}_3$

D. P. Belozorov,¹ T. V. Kalmykova,² S. I. Tarapov,² A. M. Pogorily,³ A. I. Tovstolytkin,³ A. G. Belous,⁴ and S. A. Solopan⁴

¹*Institute for Theoretical Physics NSC "Kharkov Institute of Physics & Technology" NAS of Ukraine, 1 Akademicheskaja St., Kharkov 61108, Ukraine*

²*Institute of Radiophysics and Electronics NAS of Ukraine, 12 Proskura St., Kharkov 61085, Ukraine*

³*Institute of Magnetism, 36-b Vernadsky Blvd., Kyiv 03142, Ukraine*

⁴*Institute of General and Inorganic Chemistry, 32/34 Palladina Blvd., Kyiv 03142, Ukraine*

(Received 15 August 2011; accepted 10 April 2012; published online 24 April 2012)

The left-handed features of Sr doped manganite lanthanum ceramics $\text{La}_{0.775}\text{Sr}_{0.225}\text{MnO}_3$ in the vicinity of its Curie temperature are studied. The left-handed features are responsible for appearance of the additional transparency peak in the forbidden band of the photonic crystal bounded with the above manganite. The magnitude of the critical exponent β ($\beta \sim 0.50$) determined in the work agrees with results reported in the literature and allows supposing that long-range interactions play an important role in the phase transition from conductive ferromagnetic to nonconductive dielectric paramagnetic state of the manganite in its Curie point.

© 2012 American Institute of Physics. [<http://dx.doi.org/10.1063/1.4705729>]

Interest to studies of left-handed media^{1–3} is provoked by possible potentiality of their application in a number of modern technologies: nanotechnology, high frequency technologies of electron-controllable devices for GHz and THz bands. As about extra high frequency (EHF) band one of the most promising substances is Sr doped manganite of lanthanum $\text{La}_{0.775}\text{Sr}_{0.225}\text{MnO}_3$ with perovskite structure.^{3,4} At definite conditions³ in microwave frequency band, this substance behaves as left-handed medium. In particular, the backward wave appears in this frequency band. If such substance is placed at the boundary of photon crystal (PC), a known Tamm peak appears in the forbidden band of the crystal accompanied with a new transmission peak, so named double negative peak (DNG peak³), the last is connected with transition of the doped manganite to transparent left-handed state.

We have already studied¹¹ in details the DNG state in $\text{La}_{0.775}\text{Sr}_{0.225}\text{MnO}_3$. Namely, it was shown that at a wide frequency band ($f < f_p$), the permittivity is negative and is described by Drude-like formula $\varepsilon = 1 - \frac{f_p^2}{f^2}$, where $f_p = 40.95$ GHz. It was also illustrated that a special type of refraction characteristic for left-handed media exists in DNG state. This refraction is characterized by negative refractive index and consequently the permeability is also negative. Therefore, effective permittivity and permeability of such medium become negative at these conditions. The negative permeability of the ferromagnet is known to appear in the vicinity of the ferromagnetic resonance (FMR), so the frequency of the double negative peak is close to FMR frequency and depends in particular from the saturation magnetization of doped lanthanum manganite. This enabled us to obtain the temperature dependence of the magnetization in the temperature range 270–400 K, where phase transition^{5,6} from metallic ferromagnetic to dielectric paramagnetic state takes place. The magnitude of the critical exponent β ($\beta \sim 0.50$) determined in the work agrees with results reported in literature and allows supposing that long-range interactions

play an important role in the phase transition from conductive ferromagnetic to nonconductive dielectric paramagnetic state of the manganite in its Curie point.

The experimental method was described in details in Refs. 3 and 6. Here, we dwell only on some special features important for our problem in consideration. The one dimensional photonic crystal (1D PC) is built from eight double cells. Each cell consists of teflon ($\varepsilon_T = 2.06$, $d_T = 1.1$ mm thick) and quartz ($\varepsilon_Q = 4.5$, $d = 1.9$ mm thick) layers.

The material $\text{La}_{0.775}\text{Sr}_{0.225}\text{MnO}_3$ has a perovskite crystal structure.⁵ A special feature of the material is the phase transition from ferromagnetic metal to paramagnetic dielectric state. The temperature of the phase transition (the Curie temperature T_C) depends on dopant concentration and can be changed with this concentration. In the considered here ceramic specimen of $\text{La}_{0.775}\text{Sr}_{0.225}\text{MnO}_3$ T_C is above the room temperature ($T_C = 350$ K).^{7,8} Note that so high T_C is very important for many practical applications of the substance.

We used the studied substance $\text{La}_{0.775}\text{Sr}_{0.225}\text{MnO}_3$ as a boundary³ (boundary interface) of the PC. The whole structure was embedded in the single-mode 8 mm waveguide. Parameters of the PC were calculated according the known method^{3,6} in order that its forbidden band lies in the interesting frequency range 20–37 GHz and the transition peak (Tamm peak) was approximately in the middle of the forbidden band.

Representative transmission spectrum recorded for the studied system of photonic crystal bounded with $\text{La}_{0.775}\text{Sr}_{0.225}\text{MnO}_3$ contains two peaks (e.g., see Fig. 2(c) in Ref. 3). The first is a Tamm-peak, which corresponds to surface oscillations—electromagnetic analog of electron Tamm states in metal.^{3,6} The frequency of Tamm-peak does not depend on external magnetic field oriented parallel to the plane of manganite plate (normal to PC axis). In addition, the second peak exists in the spectrum. This peak,³ known as a DNG-peak, is formed in the frequency region where both permittivity and permeability of the boundary

medium—manganite-perovskite—become negative. This peak corresponds to existence of the backward wave in the left-handed boundary medium.

It is important that the DNG-peak changes its position sideways to higher frequencies when the external magnetic field increases. The change is practically linear and depends on the temperature. In particular, the dependence $f_{DNG}(H)$ moves to high frequency side as the temperature increases. When the temperature $T = 350$ K is approached, the DNG-peak intensity decreases sharply in its vicinity and at $T > 350$ K the DNG-peak disappears practically completely (Fig. 1(a)).

The observed behavior evidently follows from the fact^{3,7,8} that at temperatures below $T_C = 350$ K, a specimen of $\text{La}_{0.775}\text{Sr}_{0.225}\text{MnO}_3$ is a metallic ferromagnet (Fig. 1(b)), but above T_C it converts into the phase of paramagnetic dielectric.^{9,10} It is evident that in paramagnetic phase the appearance of left-handed properties of the substance is excluded.

As it was shown in Refs. 3 and 11, the DNG-peak appears in ferromagnetic manganite-perovskite specimen at definite values of magnetic field, which corresponds to negative permeability of the substance.

In turn, negativity of the permittivity is connected with metallic conductivity of the specimen Drude-like model. As

about negativity of permeability, it was stated above, that it occurred in the field region above FMR-peak for the fields which exceeds the FMR resonance frequency.

Therefore, as the magnetic field increases, the frequency of the DNG-peak (together with the frequency of the FMR-peak) moves to the region of higher frequencies (Fig. 2(a) (Ref. 11)). The FMR frequency is determined by well-known Kittel formula, which connects resonance frequency-field characteristics of magnet with its parameters:

$$hf_{\text{res}} = g\beta\sqrt{H_{\text{res}}(H_{\text{res}} + 4\pi M_s)}, \quad (1)$$

where f_{res} is the resonant frequency, h is the Plank constant, H_{res} is the resonant field, g is the factor of spectroscopic splitting, and M_s is the saturation magnetization. As the temperature increases and approaches the Curie temperature, the value of saturation magnetization M_s decreases. In this case, the FMR-peak and simultaneously the DNG-peak move to the region of higher magnetic fields. Resonance frequency-field curves also move to the region of higher fields. Near the Curie temperature, the magnetization tends to zero and the position of resonance frequency-field curves cease to depend

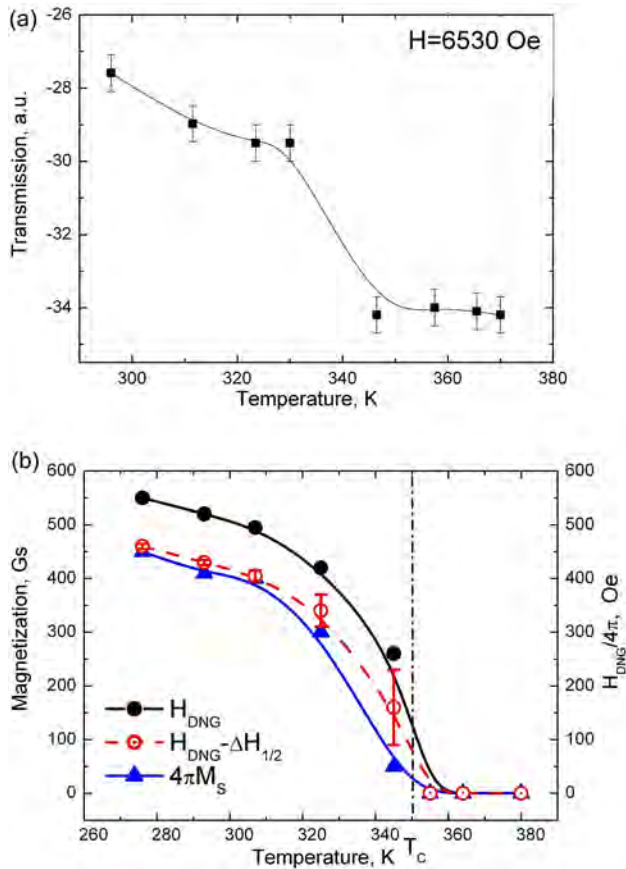


FIG. 1. (a) The typical dependence of peak intensity on the temperature for some given field value ($H = 6530$ Oe). (b) Temperature dependence of the magnetization of $\text{La}_{0.775}\text{Sr}_{0.225}\text{MnO}_3$ specimen: open circles—the magnetization of the specimen determined with the help of the DNG-peak; triangles—the magnetization determined with independent method; closed circles—the field position of the DNG-peak.

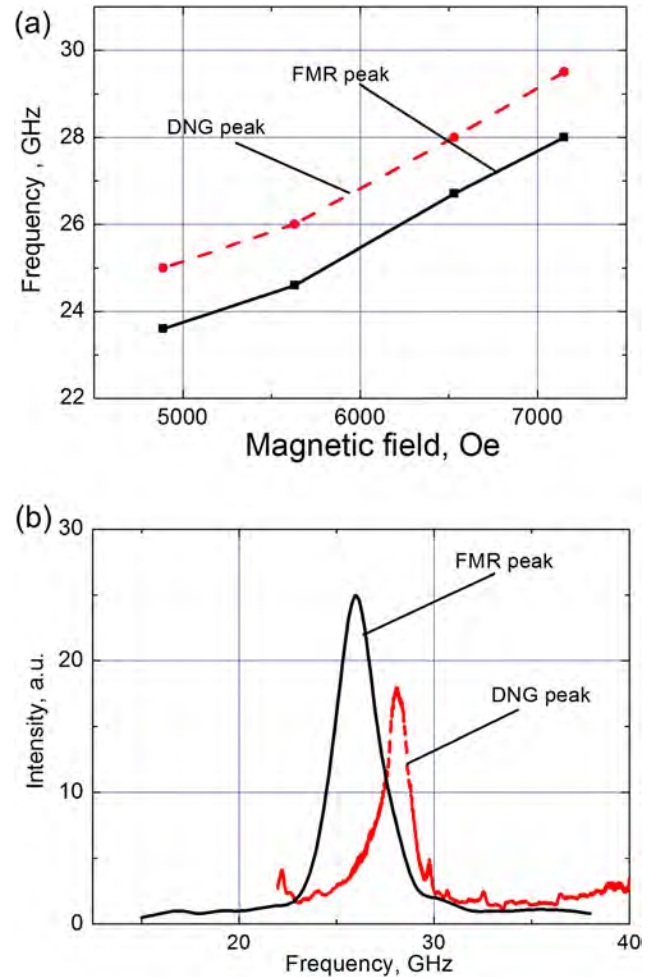


FIG. 2. (a) FMR absorption peak (black solid line) and the DNG peak at the same field values (red dashed line). (b) The positional relationship of both peaks for various frequencies. The DNG peak is always situated at the right (high-frequency) side of the FMR peak, where the real part of permeability is negative.

on the temperature. Besides as the specimen converts to the paramagnetic state, its permeability becomes positive for any field in the vicinity of the magnetoresonance peak. Therefore, the conditions of manganite-perovskite left-handed properties are violated at $T > T_C$. Note here that non-zero value of conductivity of the boundary interface of the photonic crystal (in our case of the specimen under study)² is the condition of the Tamm-peak existence, consequently after the phase transition the Tamm-peak also disappears.

Based on data of Fig. 1(b), we can estimate the values of saturation magnetization of the specimen. We should take into account that the experimental frequency of the DNG-peak belongs to high frequency wing of the FMR-peak and exceeds the central frequency of the FMR-peak by approximately half of the linewidth (δH) of FMR-peak. From independent FMR measurements, we obtain the value of this magnitude to be equal to $\delta H \approx 600$ Oe. Extracting from the field corresponding to the value of DNG-peak (Fig. 1(b), the closed circles), we obtain the value of the FMR field (Fig. 1(b), the open circles). Then with the help of Kittel formula (1), we can determine the value of saturation magnetization entering the formula and corresponding to given temperature.

Some details concerning the measured relative positions of the FMR and the DNG peaks should be mentioned here (see Figs. 2(a) and 2(b)).

The magnetization determined with the help of the DNG-peak was then compared in the same temperature range with the saturation magnetization of the specimen of Sr doped lanthanum manganite $\text{La}_{0.775}\text{Sr}_{0.225}\text{MnO}_3$. We recorded the FMR-peak for the specimen and then using Kittel formula, we determined the value of the saturation magnetization. The temperature dependence of the magnetization is shown in Fig. 1(b) with triangles. As can be seen from this figure, the values of the saturation magnetization determined with two methods (using the DNG-peak and the FMR resonance) are in close agreement. This makes it possible to suggest about the FMR frequency corresponding to the DNG-peak and consequently about left-handed medium existing in the system under consideration.

Note that errors in the data obtained from the DNG peak field-position increase as the temperature tends to T_C . This takes place because the amplitude of the DNG peak decreases drastically in this temperature range (see Fig. 1(a)).

According to the literature, the temperature dependence of magnetization near the Curie point has the form $M = (1 - T/T_C)^\beta \cdot M_0$, but the magnitude of the critical index β depends on the state of strontium doped lanthanum manganite: for the monocrystal¹² this exponent equals $\beta \sim 0.37$ (the model of Heisenberg) while for the polycrystal^{13,14} $\beta \sim 0.5$ (closely agree with the mean-field model). In our case of doped ceramic manganite specimen as can be seen from Fig. 3, the critical exponent β is close to 0.50. Therefore, the behavior of our specimen at magnetic phase transition is close to the behavior of polycrystal, for which the effective mean-field approximation is valid. As it takes place for the polycrystal, the significant role of long-range interactions can also be the reason for such behavior of ceramic manganite. Note that in the lanthanum manganite, the

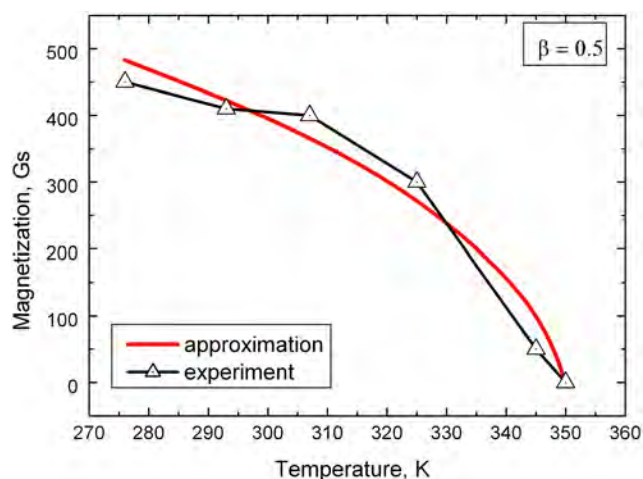


FIG. 3. The approximation of magnetization-temperature dependence with the formula $M = (1 - T/T_C)^\beta \cdot M_0$, for $\beta = 0.50$.

phase transition in its Curie point is accompanied also with the phase transition in electron system: the metal-insulator transition at the Curie temperature.

To conclude, we state that obtained experimental findings concerning magnetization of doped manganite-perovskite $\text{La}_{0.775}\text{Sr}_{0.225}\text{MnO}_3$ support the conclusion about left-handedness of its electro-dynamical properties in the millimeter wave band.

From the analysis of experimental data it follows also that:

1. temperature dependence of the magnetization obtained from DNG-peak frequency position is characteristic for the transition ferromagnet-paramagnet near the Curie temperature T_C ;
2. intensity of the DNG-peak decreases sharply near the Curie temperature and disappears above this temperature;
3. values and temperature dependence of the magnetization determined with the DNG-peak agree closely with the magnetization determined by the FMR method. The fact suggests that the negativity of the permeability at frequencies corresponding to the DNG-peak and supports once more the left-handed properties of the given Sr doped lanthanum manganite;
4. temperature dependence of the magnetization in the vicinity of Curie point suggests the conclusion that the mean-field approximation is true for ceramic specimen of Sr doped lanthanum manganite.

¹J. B. Pendry and D. R. Smith, *Phys. Today* **57**, 37 (2004).

²A. Pimenov, A. Loidl, K. Gehrke, V. Moshnyaga, and K. Samwer, *Phys. Rev. Lett.* **98**, 197401 (2007).

³M. K. Khodzitsky, T. V. Kalmykova, S. I. Tarapov, D. P. Belozorov, A. M. Pogorily, A. I. Tovstolytkin, A. G. Belous, and S. A. Solopan, *Appl. Phys. Lett.* **95**, 082903 (2009).

⁴R. W. Ziolkowski and E. Heyman, *Phys. Rev. E* **64**, 056625 (2001).

⁵A. I. Tovstolytkin, A. M. Pogorily, D. I. Podyalovskii, V. M. Kalita, A. F. Lozenko, P. O. Trotsenko, S. M. Ryabchenko, A. G. Belous, O. I. V'yunov, and O. Z. Yanchevskii, *J. Appl. Phys.* **102**, 063902 (2007).

⁶S. Chernovtsev, D. Belozorov, and S. Tarapov, *J. Phys. D: Appl. Phys.* **40**, 295–299 (2007).

- ⁷A. I. Tovstolytkin, A. N. Pogorily, A. I. Matviyenko, A. Ya. Vovk, and Zh. Wang, *J. Appl. Phys.* **98**, 043902 (2005).
- ⁸K. Ghosh, C. J. Lobb, R. L. Greene, S. G. Karabashev, D. A. Shulyatev, A. A. Arsenov, and Y. Mukovskii, *Phys. Rev. Lett.* **81**, 21 (1998).
- ⁹A. G. Belous, O. I. V'yunov, E. V. Pashkova, O. Z. Yanchevskii, A. I. Tovstolytkin, and A. N. Pogorily, *Inorg. Mater.* **39**(2), 161 (2003), translated from *Neorganicheskie Materialy* **39**(2), 212 (2003).
- ¹⁰A. I. Tovstolytkin, A. M. Pogorily, A. I. Matviyenko, A. Y. Yovk, and Zh. Wang, *J. Appl. Phys.* **102**, 043902 (2005).
- ¹¹M. K. Khodzitsky, S. I. Tarapov, D. P. Belozorov, A. M. Pogorily, A. I. Tovstolytkin, A. G. Belous, and S. A. Solopan, *Appl. Phys. Lett.* **97**, 131912, (2010).
- ¹²K. Ghosh, C. J. Lobb, R. L. Greene, S. G. Karabashev, D. A. Shulyatev, A. A. Arsenov, and Y. Mukovskii, *Phys. Rev. Lett.* **81**, 23 (1998).
- ¹³Ch. V. Mohan, M. Seeger, H. Kronmüller, P. Murugaraj, and J. Maier, *J. Magn. Magn. Mater.* **183**, 348 (1998).
- ¹⁴N. V. Khiem, P. T. Phong, L. V. Bau, D. N. H. Namb, L. V. Hong, and N. X. Phuc, *J. Magn. Magn. Mater.* **321**, 2027 (2009).